1987ApJ...320..825L

THE ASTROPHYSICAL JOURNAL, 320:825–841, 1987 September 15
© 1987. The American Astronomical Society. All rights reserved. Printed in U.S.A.

CO OBSERVATIONS OF *IRAS* SOURCES WITH 11.3 MICRON SILICON CARBIDE DUST FEATURES[1]

D. A. LEAHY, SUN KWOK, AND R. A. ARQUILLA
Department of Physics, The University of Calgary
Received 1986 December 26; accepted 1987 March 16

ABSTRACT

We report the detection of CO emission from seven late-type stars selected from the sources observed by the *IRAS* Low Resolution Spectrometer to have 11 μm SiC features. All these sources have no existing catalog associations and are typically 10 times weaker at 12 μm than previously detected radio carbon stars. We view them as being excellent candidates for hitherto unidentified carbon stars. Comparison of these objects with IRC +10216 suggests that the distance to IRC +10216 may have been overestimated in the past.

Subject headings: infrared: sources — interstellar: grains — stars: carbon — stars: circumstellar shells

I. INTRODUCTION

The 11.3 μm dust feature was discovered by Treffers and Cohen (1974) in emission in late-type stars and is generally believed to be due to silicon carbide (SiC) grains in the circumstellar envelope. The presence of this feature, rather than the 9.7 μm silicate feature, is an indication of the carbon richness (C/O > 1) of the circumstellar envelope (Merrill and Ridgway 1979). Another manifestation of the carbon-rich circumstellar envelope is line emissions due to rotational transitions of CO molecule (Knapp *et al.* 1982). Among the 136 evolved stars detected to have circumstellar CO emission, ~50% are found to be carbon-rich. Since the fraction of carbon stars among evolved giants in the Galaxy is usually assumed to be small (<10%), the high CO detection probability in carbon stars can in part be attributed to the higher carbon abundance in the envelope (Knapp 1987).

The recently-released Low Resolution Spectra (LRS) Catalog (*IRAS* Science Team 1986) of the *Infrared Astronomical Satellite* (*IRAS*) lists 539 objects with the 11.3 μm SiC feature. These sources have LRS characterizations (LRSCHAR) of 41–49, with the second digit indicating the strength of the 11.3 μm feature. While some of the class 40 objects can be associated with known variable stars, a significant number have no association with existing star catalogs. The IRC and AFGL infrared sky surveys have discovered many carbon stars with thick circumstellar envelopes and low color temperatures (the most famous example being CW Leo = IRC +10216 = AFGL 1381 = IRAS 09452+1330); the LRS catalog may contain hitherto unidentified carbon stars with low color temperatures and fluxes lower than the detection limits of the previous surveys.

IRC +10216, with a color temperature of ~500 K and a pulsation period of ~600 days, is believed to be an advanced AGB star currently undergoing rapid mass loss. Its richness in carbon-based polyatomic molecules (Olofsson 1987) is probably the result of heavy elements dredged up from the stellar interior. IRC +10216 is, however, unlikely to be a unique object, and it is possible that there are more distant IRC +10216–like objects in the Galaxy. The 12.5 μm flux (F_ν) of IRC +10216 is 5×10^4 Jy which implies that a similar star at 50 times its estimated distance of 290 pc (Herbig and Zappala 1970) would still be included in the LRS catalog. Its 3′ circumstellar envelope would resemble a point source to most millimeter telescopes at a distance of 2–3 kpc, while the beam-diluted $J = 1$–0 brightness temperature ($13\ \mathrm{K} \times 10^{-2} \approx 130$ mK) would still be detectable.

We have therefore undertaken a program to search for heavily obscured carbon stars among the *IRAS* sources with the 11.3 μm SiC feature. Observations were made using the NRAO 12 m millimeter radio telescope at the 1–0 and 2–1 lines of CO. Sources with no known associations (with one exception), which have a high probability of being variable based on the *IRAS* observations at three epochs and have high 12.5 μm fluxes were chosen as candidates.

II. OBSERVATIONS

The data were taken during 1986 May using the National Radio Astronomy Observatory[2] 12 m antenna and cooled dual-polarization receivers tuned to 115 GHz ($J = 1$–0 transition) and 230 GHz ($J = 2$–1 transition). Most sources were observed at only one of these frequencies. The spectrometers were two 256 × 1 MHz filterbanks operated such that each filterbank received one polarization. The outputs of the filterbanks were then averaged to improve the signal-to-noise ratio. This arrangement resulted in velocity resolutions of 2.6 and 1.3 km s^{-1} per channel at 115 GHz and 230 GHz, respectively. Pointing and subreflection focusing corrections were determined periodically by observing Jupiter or Saturn. These corrections were small and consistent; e.g., the pointing varied by 2″ to 8″ from check to check. The planet data were also used to determine the telescope beamwidths; the 12 m beamwidths are ~55″ at 115 GHz and ~33″ at 230 GHz.

The sources were observed by switching between the source positions and off-source reference positions, which were offset 5′ or 10′ in azimuth. A single observation usually lasted 10 minutes, with total integration times per source of 40–100 minutes. The data were corrected for atmospheric absorption by a chopper wheel, and the results expressed in units of the antenna temperature T_R^* (Kutner and Ulrich 1981). Finally, the data were corrected for the beam-to-source coupling efficiency η. In the absence of detailed knowledge of the brightness distributions of our sources (except that they are likely smaller

[1] Publication of the Rothney Astrophysical Observatory, No. 44.

[2] The National Radio Astronomy Observatory is operated by Associated Universities Inc. under contract to the National Science Foundation.

© American Astronomical Society • Provided by the NASA Astrophysics Data System

1987ApJ...320..825L

TABLE 1

OBSERVATIONS

Source	R.A. (1950)	Decl. (1950)	l^{II}	b^{II}	J_U–J_L	σ (mK)
03239+6038.....	$03^h29^m21^s.6$	+60°38′20″	141	+3.9	2–1	49
17581−1744.....	17 48 11.4	−17 44 20	11	+2.6	1–0	23
					2–1	24
18369−1036.....	18 36 58.5	−10 34 53	22	−2.2	2–1	32
18424+0346.....	18 42 29.2	+03 46 25	36	+3.2	1–0	27
					2–1	32
18585+0900.....	18 58 30.2	+09 00 43	42	+2.0	2–1	47
19346+1209.....	19 34 39.1	+12 09 52	49	−4.3	1–0	17
					2–1	28
19358+0917.....	19 35 49.0	+09 17 15	47	−5.9	1–0	25
					2–1	32
19419+3222.....	19 41 56.1	+32 22 11	68	+4.3	2–1	23
19552+3142.....	19 55 13.7	+31 42 17	68	+1.5	2–1	36
20223+6935.....	20 22 18.2	+69 35 02	103	+18.0	1–0	26
20282+3604.....	20 28 12.2	+36 04 31	76	−1.7	2–1	35
20323+3153.....	20 32 22.9	+31 53 15	73	−4.9	2–1	47
20532+5554.....	20 53 15.8	+55 54 06	94	+7.1	2–1	31
21147+5110.....	21 14 45.8	+51 10 05	93	+1.6	2–1	123
21223+5114.....	21 22 21.7	+51 14 05	94	+0.8	1–0	22
					2–1	72
21265+5042.....	21 26 30.7	+50 42 17	94	−0.0	1–0	51
21449+4950.....	21 44 56.2	+49 50 08	95	−2.6	2–1	25
23279+5336.....	23 27 56.5	+53 36 34	111	−7.1	2–1	37

than the beam), we assume that $\eta \approx \eta_{MB}$, where η_{MB} is the fraction of the antenna power contained in the main beam. From our planet observations we find that $\eta_{MB} \approx 0.9$ at 115 GHz and $\eta_{MB} \approx 0.6$ at 230 GHz.

III. RESULTS

The observed *IRAS* sources are listed in Table 1 together with their positions, galactic coordinates, the CO transition being observed, and the rms noise in the final observed spectrum. The source positions are taken from the *IRAS Point Source Catalog* and are generally accurate to within 15″ (Hrivnak, Kwok, and Boreiko 1985). The final observed spectrum consisted of the sum of all the edited scans for the source for the appropriate CO transition with a baseline removed which was either a first-order or third-order polynomial. The calculation of the rms was performed with any observed lines removed.

Table 2 contains a list of the observed line parameters for the seven sources toward which we see evidence of broad CO emission lines (see also Figs. 1*a*–1*j*). The columns in Table 2 refer to (1) the source name; (2) the transition detected; (3) the antenna temperature of the line peak T_R*; (4) the velocity of the line centroid, V_0; (5) the line width at half-maximum intensity ΔV; and (6) the line width at zero intensity ΔV_z. Except where indicated, T_R*, V_0, and Δ_V are obtained from Gaussian fits to the unsmoothed spectra; ΔV_z is measured directly from hardcopy of the spectra. While the profile of an optically thick line produced by an unresolved envelope with constant expansion velocity is expected to be parabolic, the Gaussian parameters are sufficiently accurate for our present purposes given the weakness of the lines and the signal-to-noise ratio. The outflow velocity of the material from the star is given by $\Delta V_z/2$.

In Table 3 are listed derived parameters for the seven CO line sources. The 2–1 line parameters are used in all cases for the reason that the 2–1 spectra have twice the velocity resolution and higher antenna temperature. In the first column are given estimated source distances D. These values are kinematic distances obtained from the values of the system velocities, V_0, and the rotation model of Burton (1974, Fig. 4.5). In those cases where two distances were possible, the adopted distance is the smaller of the two values. For one source (20532+5554) the velocity of −0.6 km s^{-1} gives a 0.1 kpc distance, but the slightly more negative velocity of −5.0 km s^{-1}, also consistent with the observed spectrum of Fig. 1*f*, gives a 1.2 kpc distance. Therefore for this source we adopt a distance of 1 kpc, realizing the large uncertainty. Our distances are probably reliable to within a factor of less than two for the remaining sources.

The mass-loss rates $\dot{M}$ given in Table 3 are obtained from equation (5) of Knapp and Morris (1985), which assumes that the envelopes are optically thick in the CO $J = 1$–0 and $J = 2$–1 transitions and unresolved by the telescope beam. The mass-loss formula used here is:

$$\dot{M} = 7.04 \times 10^{-8} T_R^*(2\text{–}1)(\Delta V_z/2)^2 D^2 \, M_\odot \, \mathrm{yr}^{-1} . \quad (1)$$

TABLE 2

OBSERVED LINE PARAMETERS

Source (1)	J_U–J_L (2)	T_R* (mK) (3)	V_0 (km s^{-1}) (4)	ΔV (km s^{-1}) (5)	ΔV_z (km s^{-1}) (6)
17581−1744[a]	1–0	47	36.6	35	47
	2–1	64	27.3	30	39
18424+0346[b]	2–1	79	7.6	35	40
19346+1209	1–0	46	73.1	25	29
	2–1	58	70.5	15	24
20532+5554	2–1	132	−0.6	17	27
21147+5110	2–1	249	−48.8	20	23
21223+5114[c]	1–0	160	−11.8	26	26
	2–1	168	−6.7	25	30
21449+4950[a]	2–1	66	−32.3	29	40

[a] Non-Gaussian line shape; V_0 from line moment, ΔV measured directly from spectrum.

[b] Broad pedestal with 9 km s^{-1} wide line superposed.

[c] Line profile contaminated by interstellar emission and absorption.

© American Astronomical Society • Provided by the NASA Astrophysics Data System

1987ApJ...320..825L

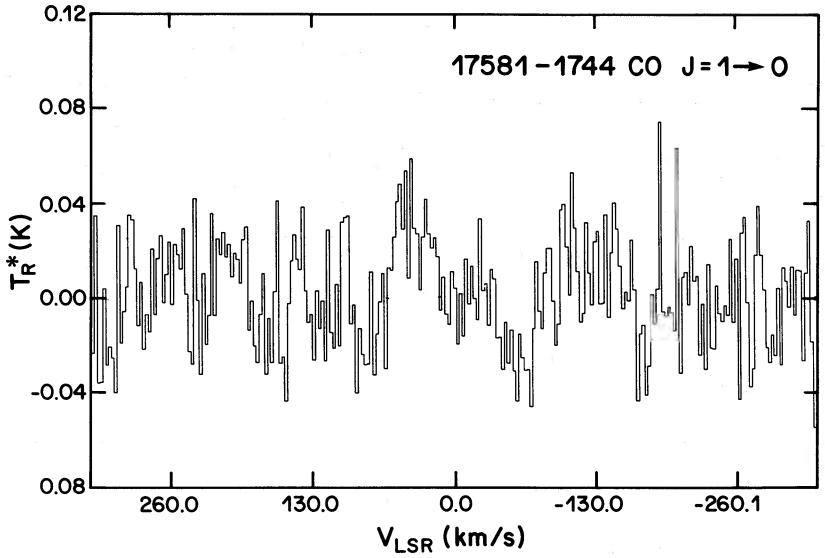

FIG. 1*a*

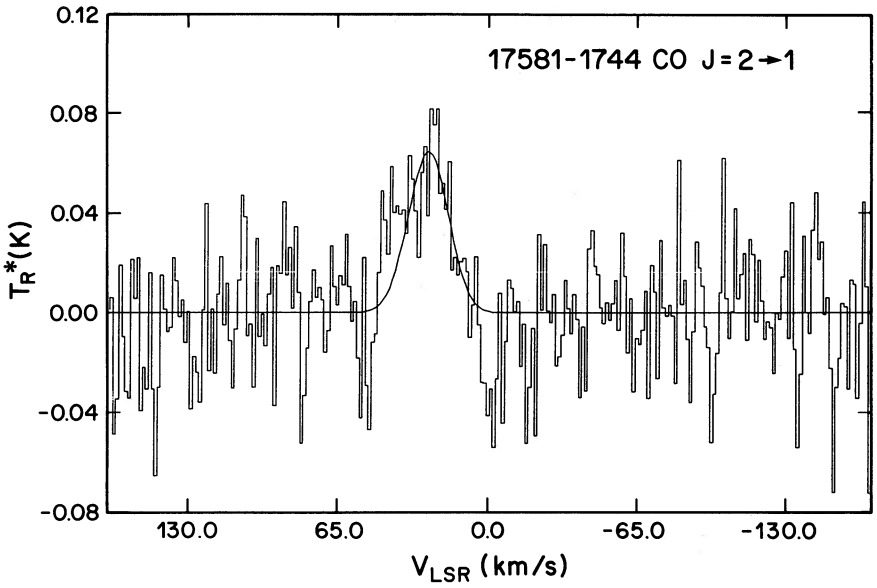

FIG. 1*b*

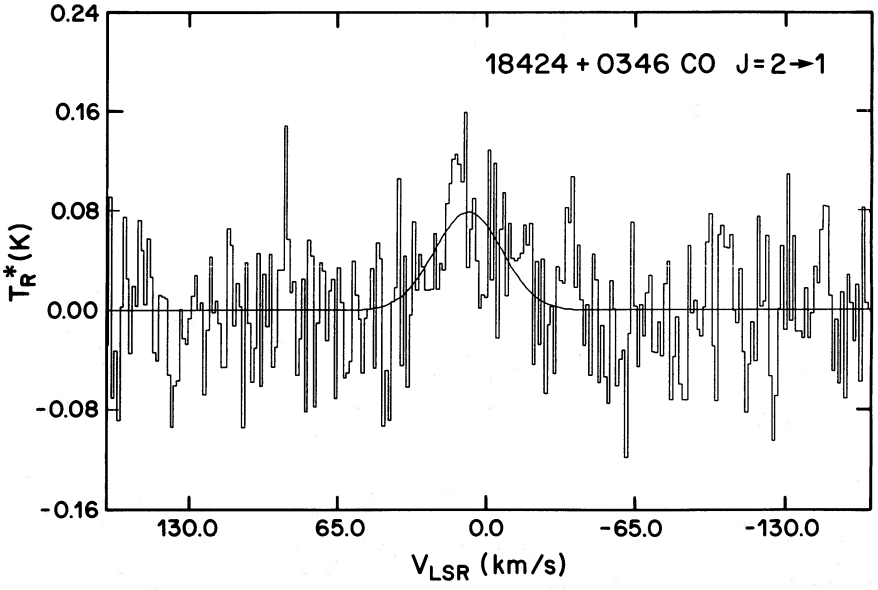

FIG. 1*c*

FIG. 1.—Observed spectra for lines listed in Table 2, labeled by the source designation and CO $J = 1$–0 or 2–1 transition observed. The antenna temperature is plotted for each channel as a function of velocity. A third-order polynomial baseline has been removed and the line fitted by a Gaussian as shown.

© American Astronomical Society • Provided by the NASA Astrophysics Data System

1987ApJ...320..825L

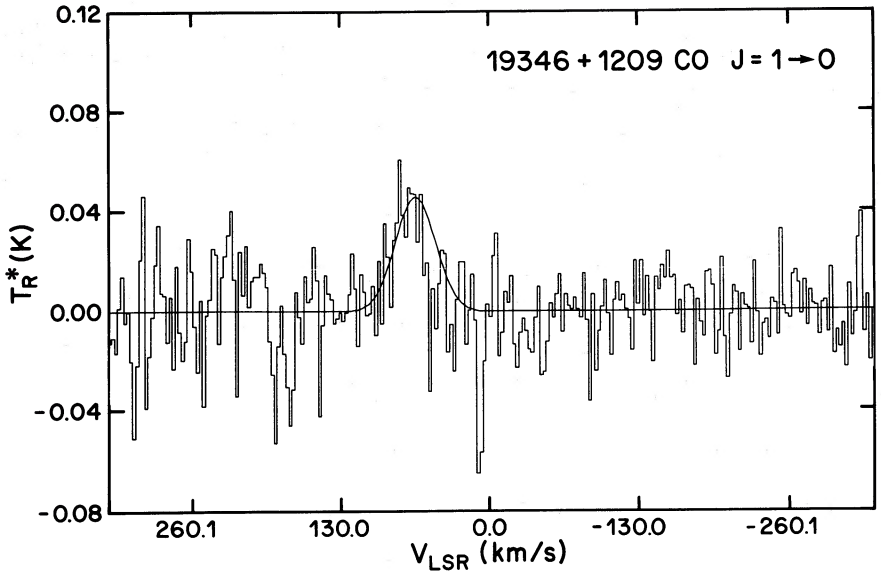

FIG. 1*d*

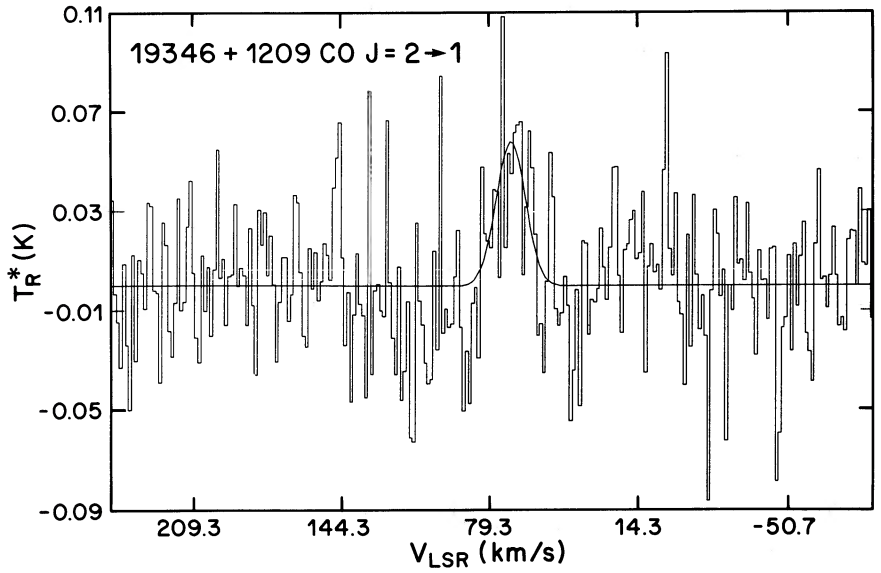

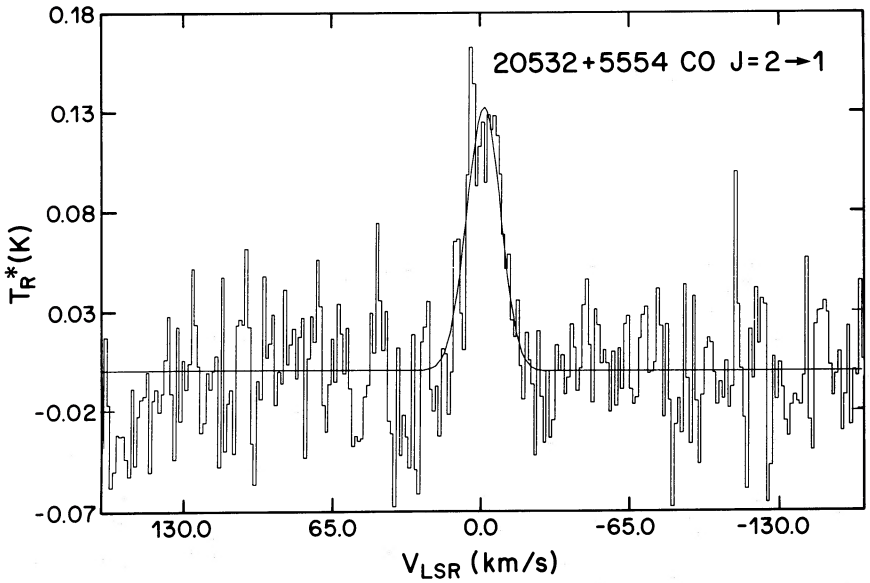

FIG. 1*f*

© American Astronomical Society • Provided by the NASA Astrophysics Data System

1987ApJ...320..825L

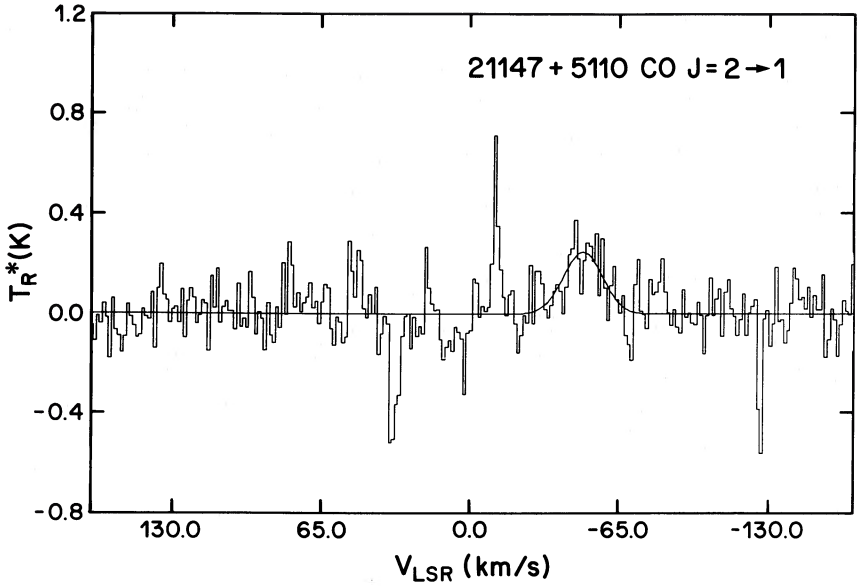

FIG. 1*g*

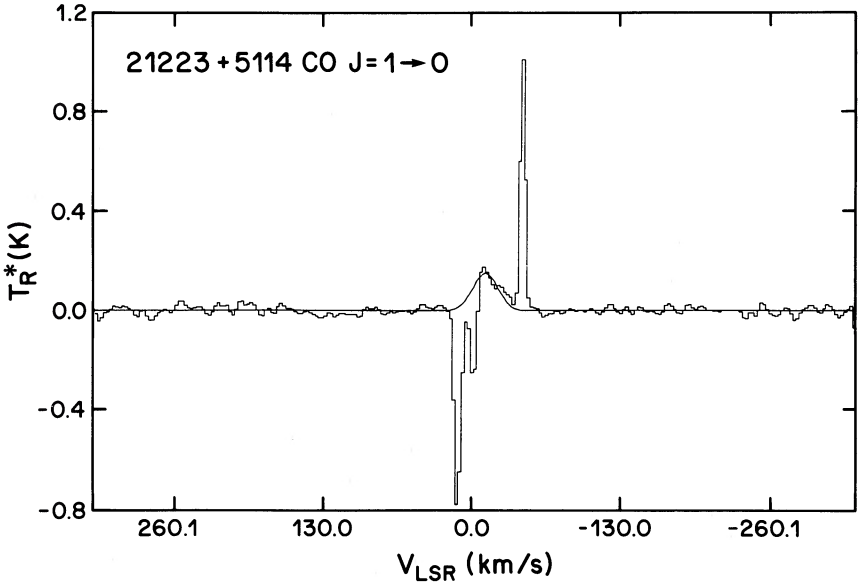

FIG. 1*h*

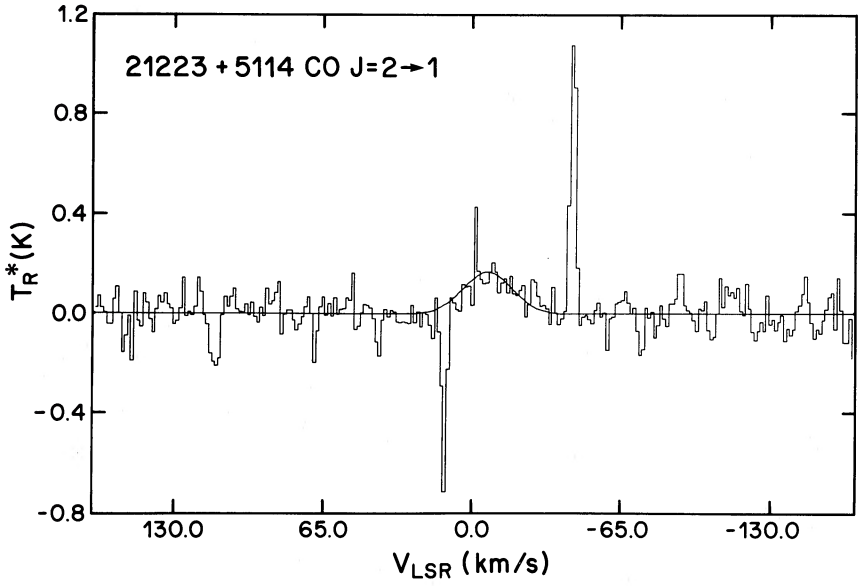

FIG. 1*i*

© American Astronomical Society • Provided by the NASA Astrophysics Data System

1987ApJ...320..825L

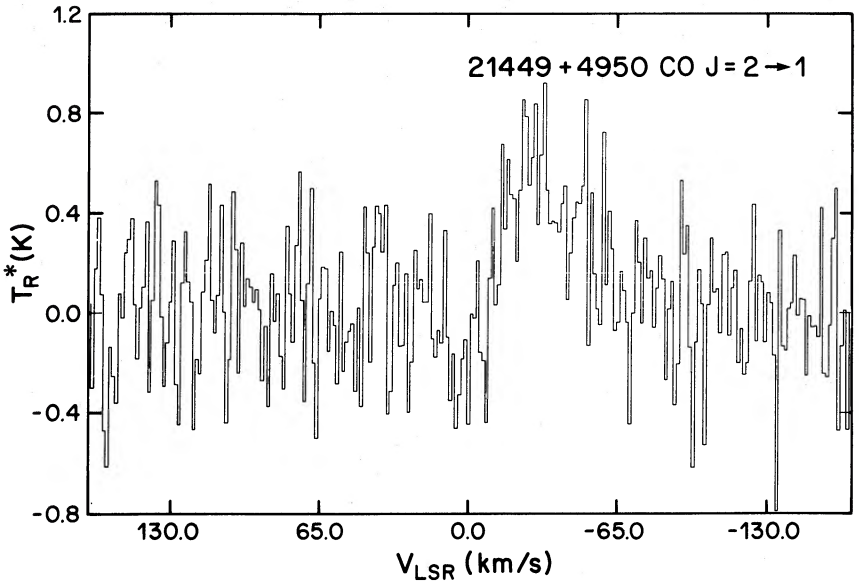

FIG. 1*j*

The distance D is in units of kpc, velocity in units of km s^{-1}, and temperature in K. We take the CO to H_2 abundance ratio to be 8×10^{-4}, appropriate to carbon-rich stars, since our sources display the SiC feature in their infrared LRS spectra. The numerical coefficient has been adjusted from Knapp and Morris (1985) by a factor of 0.42 to correct for the difference between the NRAO and Bell Labs millimeter telescopes (see Fig. 8 of Knapp and Morris). The numerical coefficient also includes a conversion factor for $T_R^*(2\text{–}1)/T_R^*(1\text{–}0)$, given by $[T_B(2\text{–}1)/T_B(1\text{–}0)][\theta(1\text{–}0)/\theta(2\text{–}1)]^2[n_x(1\text{–}0)/n_x(2\text{–}1)]$ (see Knapp *et al.* 1982). We assume intrinsic source brightness temperatures of $T_B(1\text{–}0) = 13$ K and $T_B(2\text{–}1) = 28$ K as in IRC +10216 (Kwan and Hill 1977); use the NRAO beamwidths $\theta(1\text{–}0) = 55''$, $\theta(2\text{–}1) = 33''$; and use $n_x(1\text{–}0) = 3 \times 10^3$ cm^{-3}, $n_x(2\text{–}1) = 1.4 \times 10^4$ cm^{-3} (Knapp *et al.* 1982) to get $T_R^*(2\text{–}1)/T_R^*(1\text{–}0) = 1.28$. Note that this is equal to the observed values, within uncertainties, of these ratios for the three sources detected in both lines: 17581−1744, 19346+1209, and 21223+5114. Also no case occurs where a source is observed at both frequencies with a detection in one line, either $J = 2\text{–}1$ or 1–0, and not in the other. This is confirmation that the modeling is essentially correct and that the sources are optically thick and unresolved as assumed. The inferred mass loss rates are substantial, with $\dot{M} \approx 2 \times 10^{-5}$–$10^{-4}\ M_\odot\ \mathrm{yr}^{-1}$ for four of the seven objects. It is important to note that $\dot{M}$ depends strongly on the source distance, since $\dot{M} \propto D^2$; the two nearby objects, 18424+0346 and 20532+5554, have low inferred mass-loss rates. While the stellar distances are difficult to estimate, we do not believe that erroneous distance determinations alone can explain our high values of $\dot{M}$ because the distances are probably reliable to within a factor of less than 2, leading to a factor of less than 4 uncertainty in the mass-loss rates, and because it does not seem likely that we have drastically overestimated D for *all* five of the remaining sources.

In addition to D and $\dot{M}$ in Table 3, we have listed total infrared fluxes and luminosities for the sources derived from *IRAS* data. The *IRAS Point Source Catalog* fluxes at 12, 25, 60, and 100 μm are plotted in Figures 2*a*–2*g* together with the LRS spectra. The broad-band fluxes have been color-corrected according to the procedure described by Kwok, Hrivnak, and Milone (1986). The 11.3 μm SiC feature is evident in all LRS spectra. The LRS characterization (LRSCHAR) and spectral qualities (1 = good, 2 = moderate, 3 = acceptable) for the short-waveband and long-wavebands are given in each figure. Detail descriptions of these quantities are given in the *IRAS Explanatory Supplement* (1985). Also plotted are eye-fitted blackbody curves (normalized to the 60 μm point) to the observed *IRAS* data. In all cases the *IRAS* data are well fitted by a blackbody curve. The best-fit temperatures are shown at the upper right of each figure. These values are also listed in column (5) of Table 3. Since near-infrared measurements are

TABLE 3

DERIVED STELLAR PARAMETERS

Source (1)	D (kpc) (2)	$\dot{M}$ ($M_\odot$ yr^{-1}) (3)	F_{IR} (ergs cm^{-2} s^{-1}) (4)	T_c (K) (5)	L_{IR} ($L_\odot$) (6)	Var (7)	θ_{bb} (8)
17581−1744.....	3.8	2.5 (−5)	5.1 (−8)	675	2.3 (2)	99%	0.″014
18424+0346.....	0.6	8.0 (−7)	3.0 (−8)	555	3.4 (2)	97	0.016
19346+1209.....	6.1	2.2 (−5)	1.8 (−8)	525	2.0 (4)	99	0.013
20532+5554.....	1.0	1.7 (−6)	3.7 (−8)	500	1.2 (3)	99	0.021
21147+5110.....	5.8	7.8 (−5)	3.2 (−8)	450	3.3 (4)	88	0.024
21223+5114.....	1.4	5.2 (−6)	2.6 (−8)	350	1.6 (3)	82	0.036
21449+4950.....	4.1	1.2 (−4)	3.4 (−8)	525	1.8 (4)	68	0.018

© American Astronomical Society • Provided by the NASA Astrophysics Data System

1987ApJ...320..825L

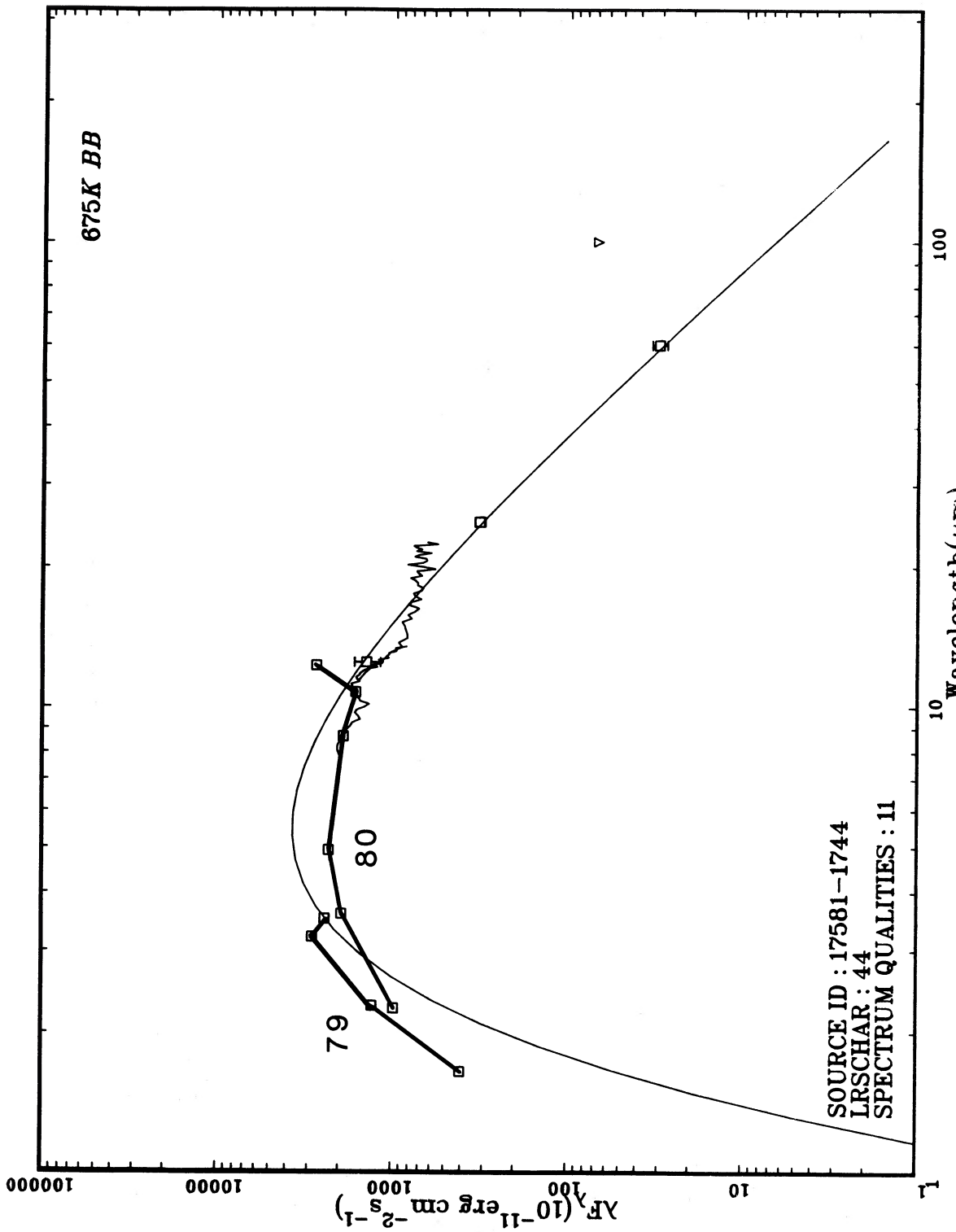

FIG. 2*a*

FIG. 2.—Infrared spectrum for each of the seven sources with detected CO line emission. *IRAS* point source catalog fluxes at 12, 25, 60, and 100 μm are shown as squares with error bars; upper limits are shown as triangles. The *IRAS* LRS spectrum is presented by two lines between 8 and 22 μm. The LRS characterization number and spectrum qualities are given at the lower left. A blackbody curve is fitted to the *IRAS* data. Note the SiC feature in the LRS spectrum at 11 μm. In Fig. 2*a* additional ground-based data of Gosnell *et al.* (1979) and Ney and Merrill (1980) are plotted as squares joined by line segments labeled 79 and 80 respectively.

© American Astronomical Society • Provided by the NASA Astrophysics Data System

1987ApJ...320..825L

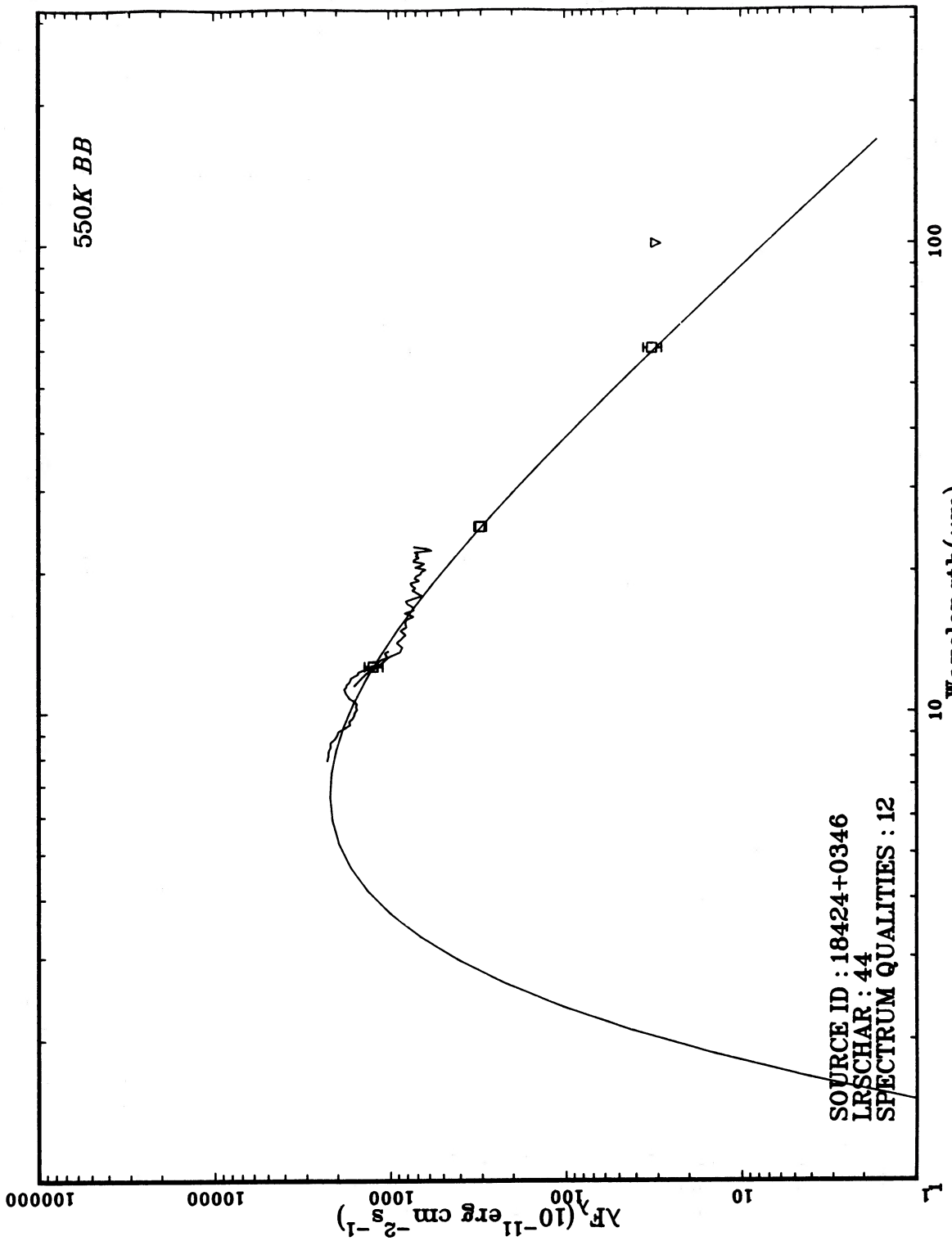

FIG. 2b

© American Astronomical Society • Provided by the NASA Astrophysics Data System

1987ApJ...320..825L

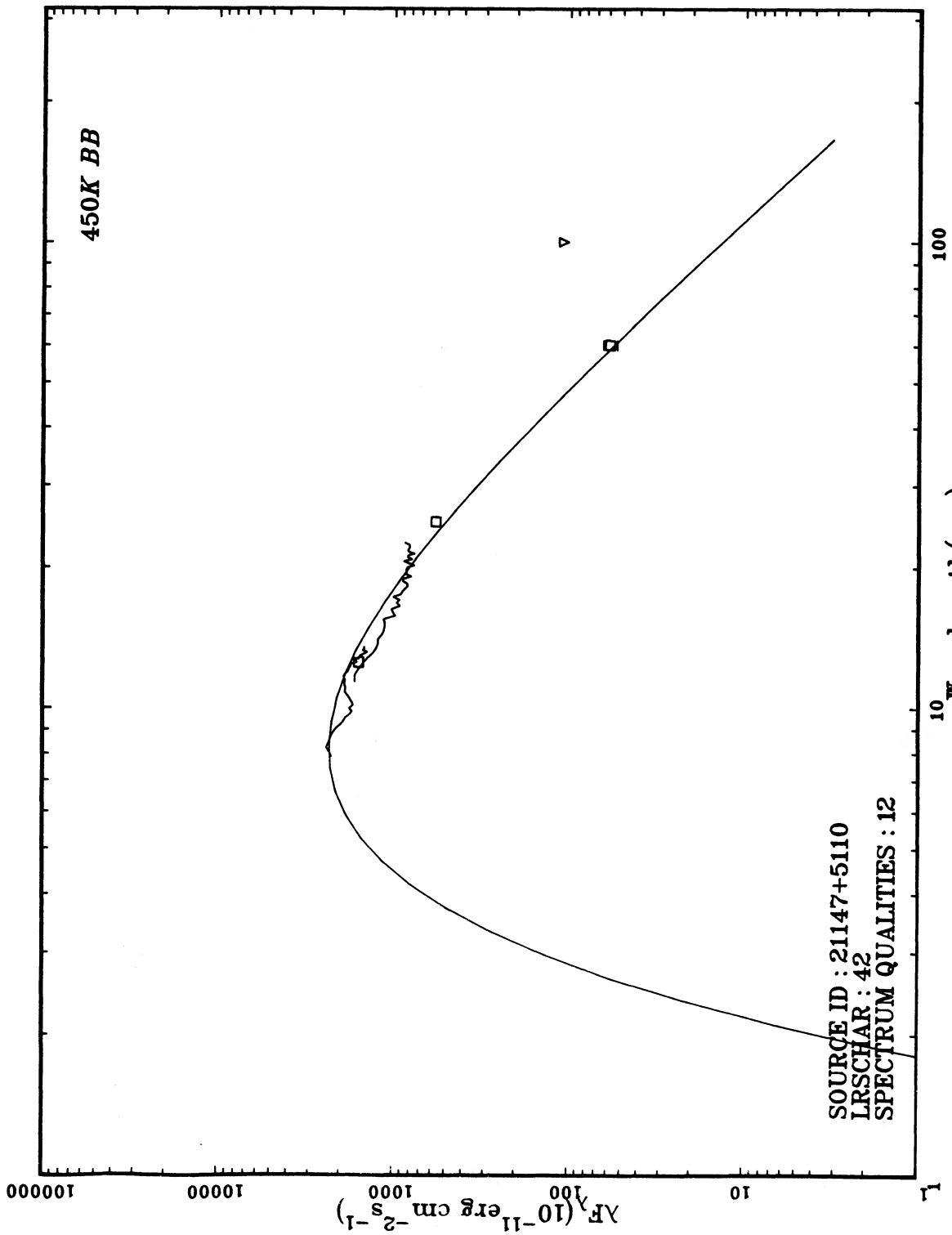

FIG. 2c

© American Astronomical Society • Provided by the NASA Astrophysics Data System

1987ApJ...320..825L

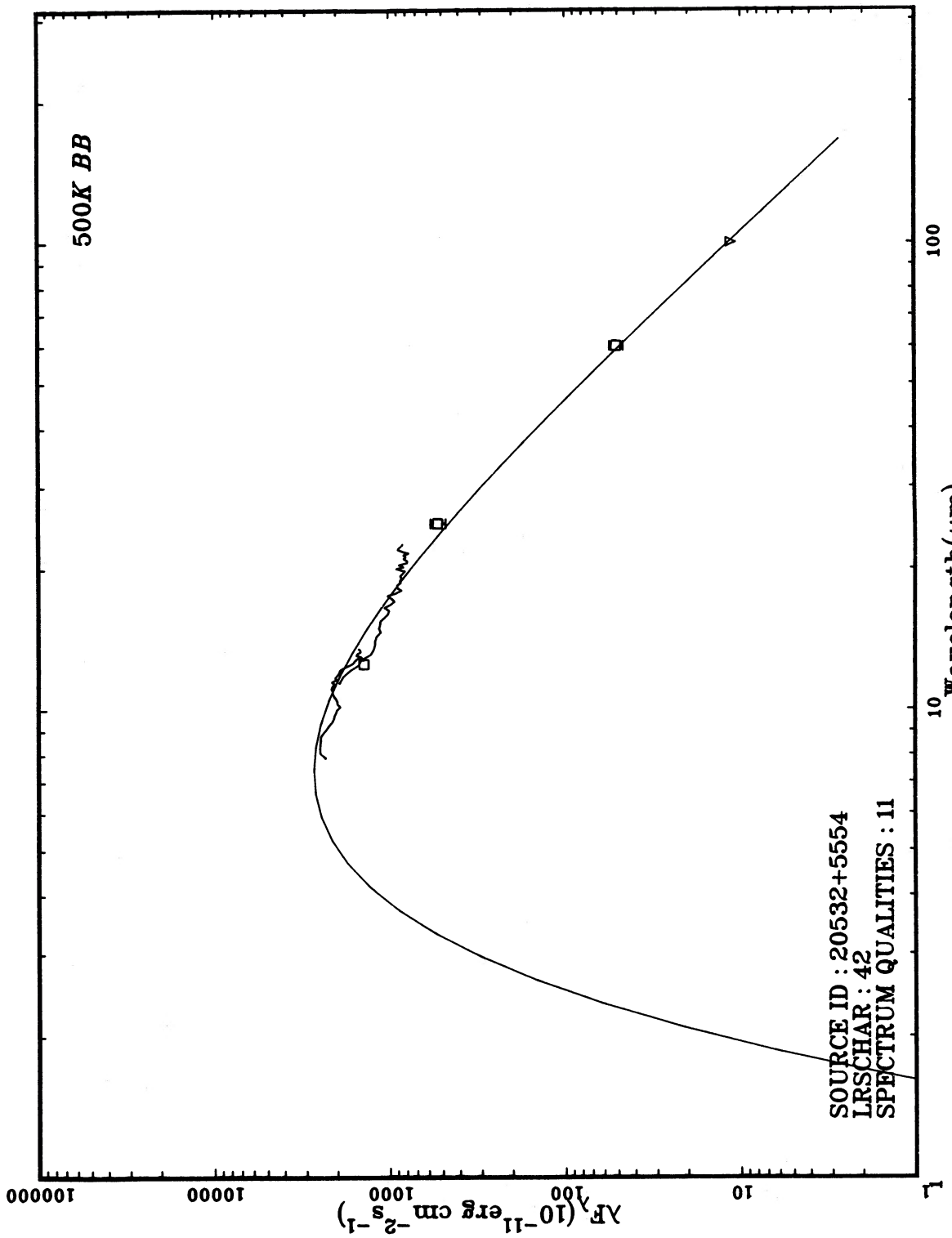

FIG. 2*d*

© American Astronomical Society • Provided by the NASA Astrophysics Data System

1987ApJ...320..825L

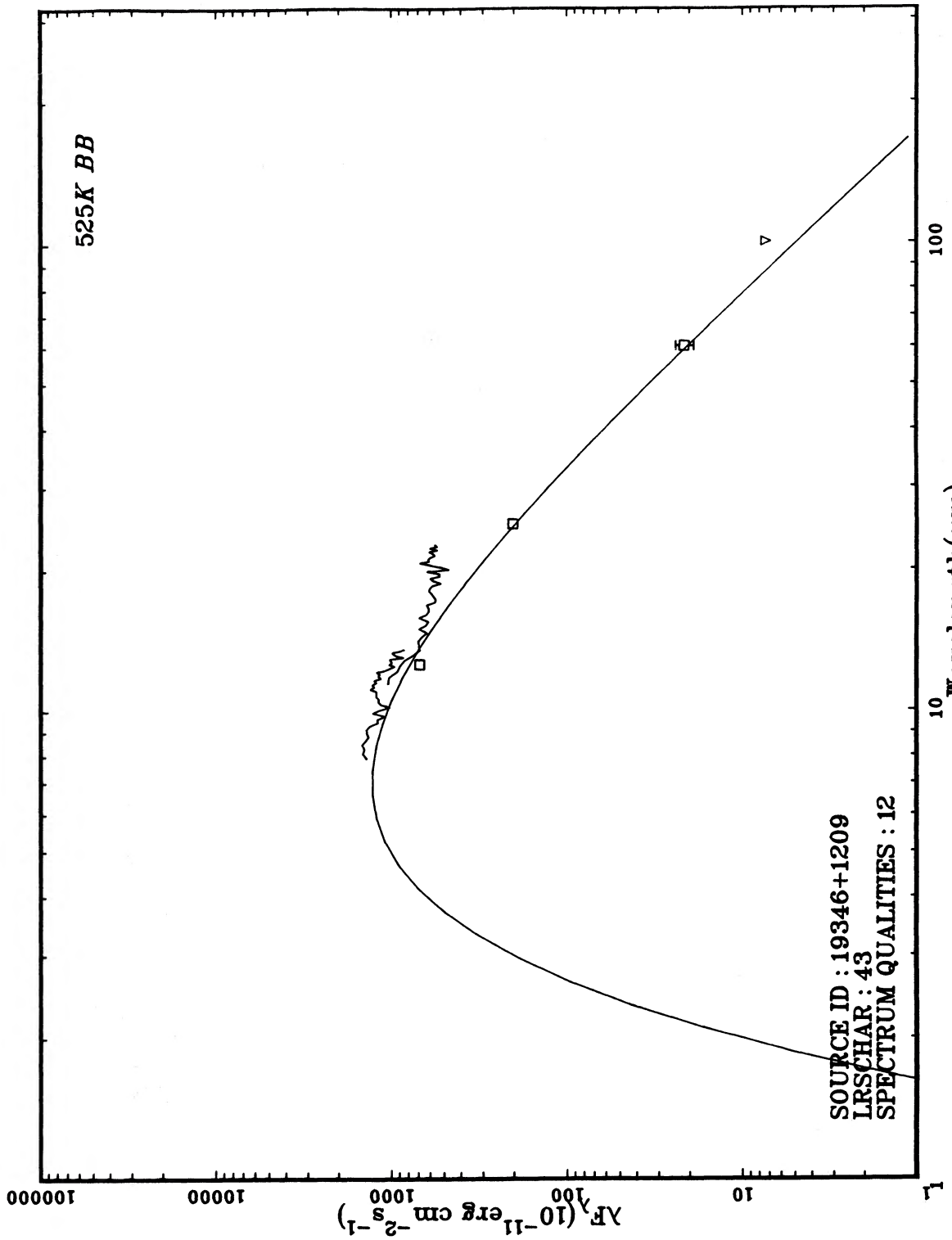

FIG. 2e

© American Astronomical Society • Provided by the NASA Astrophysics Data System

1987ApJ...320..825L

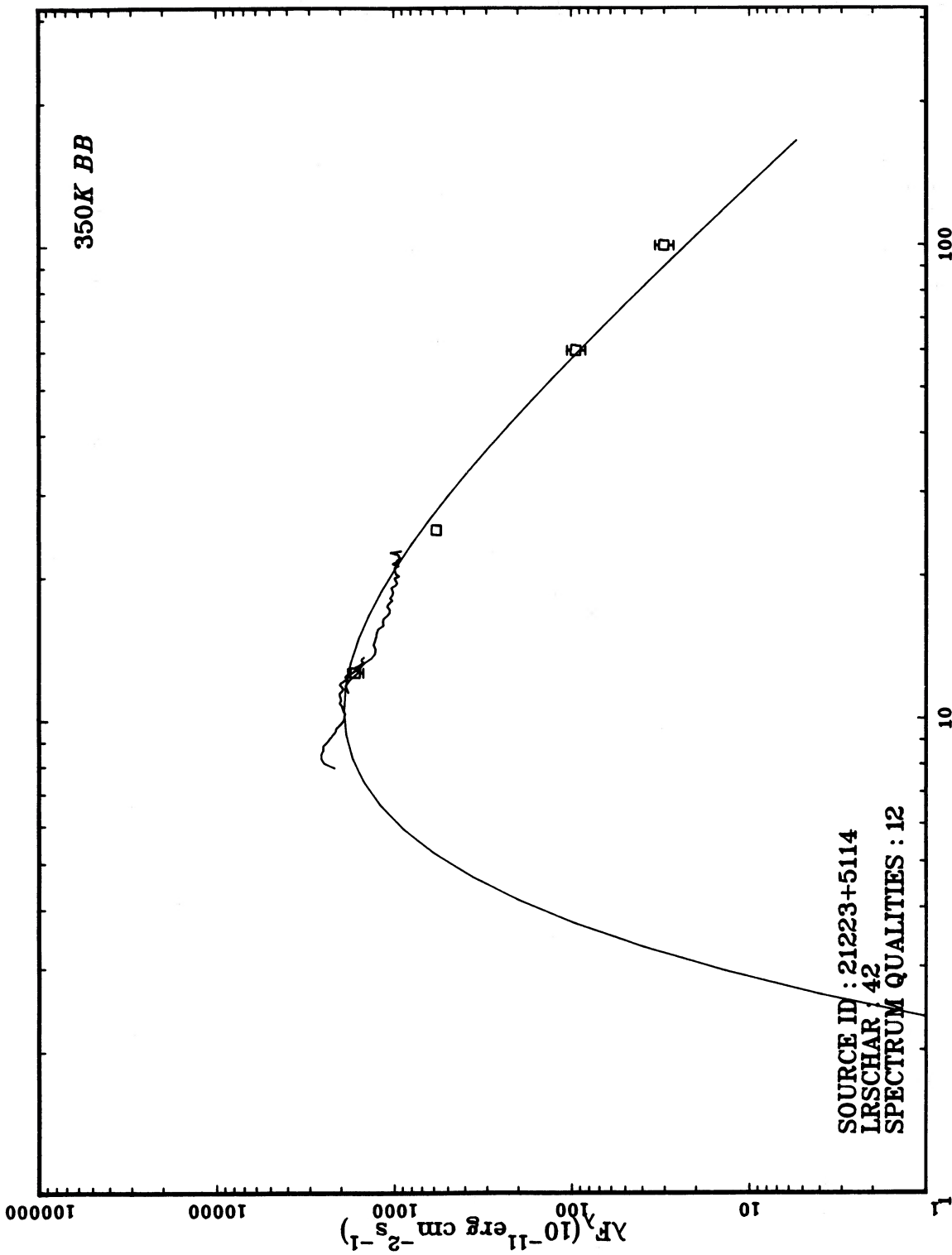

FIG. 2f

© American Astronomical Society • Provided by the NASA Astrophysics Data System

1987ApJ...320..825L

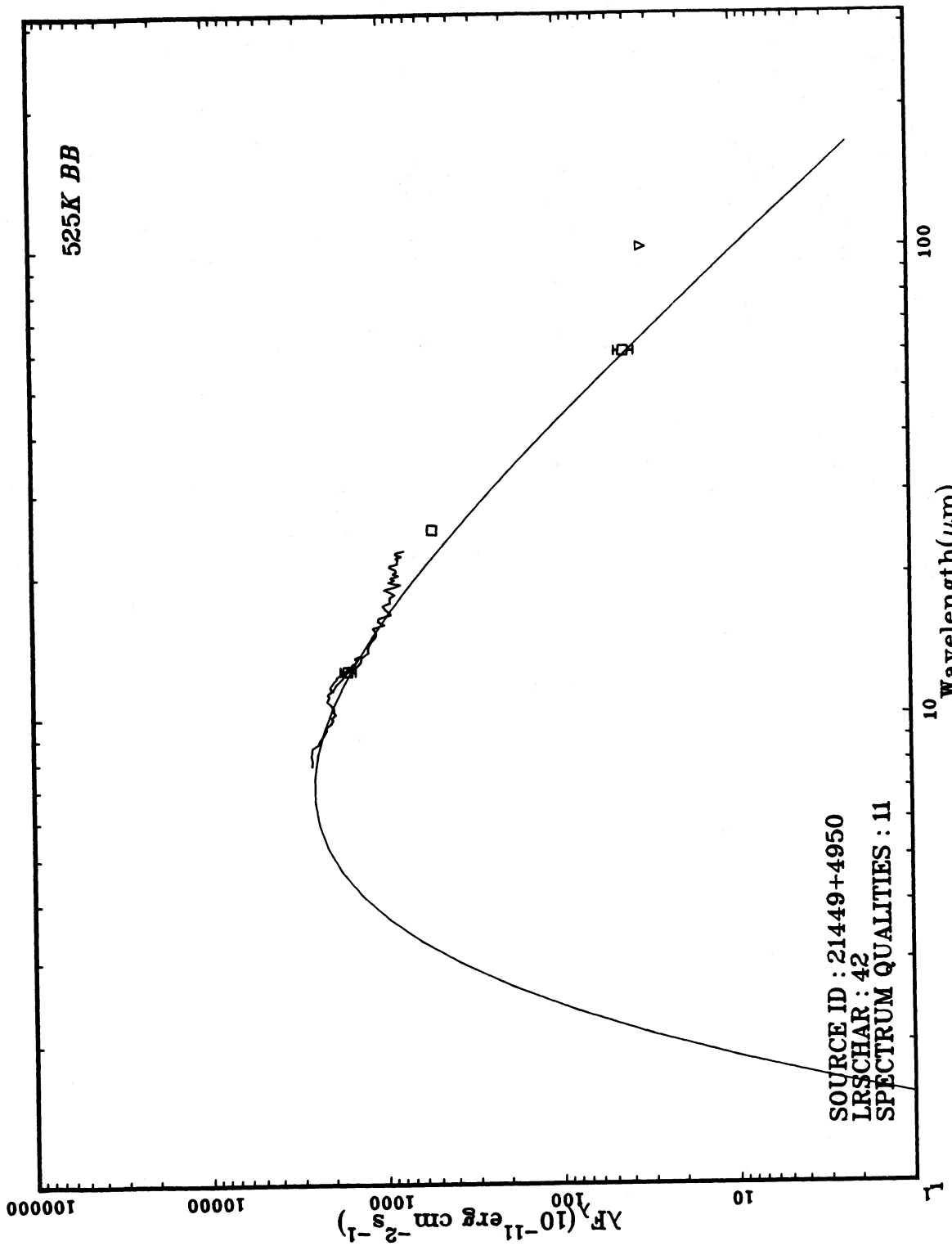

FIG. 2g

© American Astronomical Society • Provided by the NASA Astrophysics Data System

1987ApJ...320..825L

not available for most of the sources, these temperatures cannot be considered to be definitive. The infrared fluxes in column (4) are estimated from the area under the Planck curve. Assuming that the infrared flux constitutes the bulk of the total flux, the infrared luminosity in column (6) would correspond to the total radiative luminosity of the star.

Also listed in Table 3 are the blackbody sizes (θ_{bb}) of the infrared emitting region

$$\theta_{bb} = \{F_\nu/[\pi B_\nu(T_c)]\}^{1/2}, \quad (2)$$

where $\nu = c/60\ \mu$m. The small values found for θ_{bb} (corresponding to blackbody radii of 10–140 AU) suggest that the circumstellar envelopes are not optically thick at 60 μm.

Having determined mass loss rates and radiative luminosities for the seven sources, it is appropriate to address the question of whether radiation pressure can account for the observed values of mass loss rates. In Figure 3 are plotted the momentum flux into the mass flow, $\dot{M}\Delta V_z/2$, versus the momentum flux of the radiation field, L_{IR}/c. Although both quantities are sensitive to the distance, which is not well determined, the ratio is independent of D. Errors in D will move the points parallel to the line $\dot{M}\Delta V_z/2 = L_{IR}/c$. Three of the seven stars have mass loss momentum flux ~ 2 times higher than the photon momentum flux, whereas the other four show near equality. This is consistent with the results of Knapp *et al.* (1982, Fig. 17) for nearby carbon stars.

Thronson *et al.* (1987) find an empirical relationship between the CO derived mass-loss rates and the infrared excess of the following form:

$$\log(\dot{M}/M_\odot\ \mathrm{yr}^{-1}) = -4 - 0.112[F_\nu(12\ \mu\mathrm{m})/F_\nu(60\ \mu\mathrm{m})]\ . \quad (3)$$

Figure 4 shows a plot of the mass-loss rate versus the 12–60 μm flux ratio for the seven stars in this paper. While there is no apparent correlation, the data points are within the scatter of the corresponding diagram of Thronson *et al.* (1987). The only conclusion one can draw is that carbon stars with thick circumstellar envelopes (such as those in our sample) have, on the average, higher mass loss rates than optical carbon stars (Knapp and Morris 1985).

IV. NOTES ON INDIVIDUAL SOURCES

With the exception of one, all the detected sources are new infrared objects.

17581−1744.—Although the *IRAS* catalog does not list a catalog association for this object, its position is close to that of AFGL 2047. Gosnell, Hudson, and Puetter (1979) give a position of $17^h57^m59^s.3$, $-17°44'34''$ with a 17″ beam, whereas Ney and Merrill (1980) give a position of $17^h58^m11^s$, $-17°44'00''$ with a 26″ beam. Both positions are in agreement with the *IRAS* position of $17^h58^m11^s.4$, $-17°44'20''$. Previous ground-based observations have been taken from the *Catalog of Infrared Observations* (Gezari, Schmitz, and Mead, 1984) and are plotted together with *IRAS* data in Figure 2*a*. The combined spectrum confirms that AFGL 2047 and 17581−1744 are indeed the same object. The best-fit blackbody temperature is ~ 675 K, refining the upper limit of 1000 K of Gosnell, Hudson, and Puetter (1979), who also classified this object as carbon rich based on 2–4 and 8–14 μm spectrophotometry.

18424+0346.—The circumstellar CO line of this source is contaminated by the presence of a strong interstellar line at 13.9 km s^{-1}. The 1–0 transition of the interstellar component has a FWHM of 5.1 km s^{-1} and a peak antenna temperature of 560 mK, or a factor of 4 greater than the peak temperature (120 mK) of the 2–1 line. Because of this contamination problem, the detection of the circumstellar line must be viewed as tentative.

21223+5554.—Besides the 11.3 μm feature in the LRS spec-

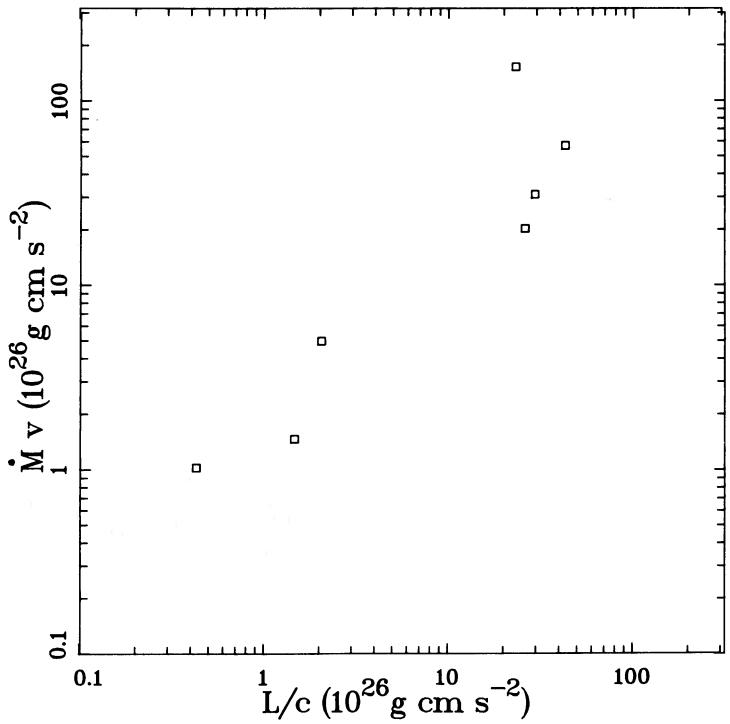

FIG. 3.—Mass-loss rate vs. infrared luminosity (L_{IR}) for the seven sources detected in CO

© American Astronomical Society • Provided by the NASA Astrophysics Data System

1987ApJ...320..825L

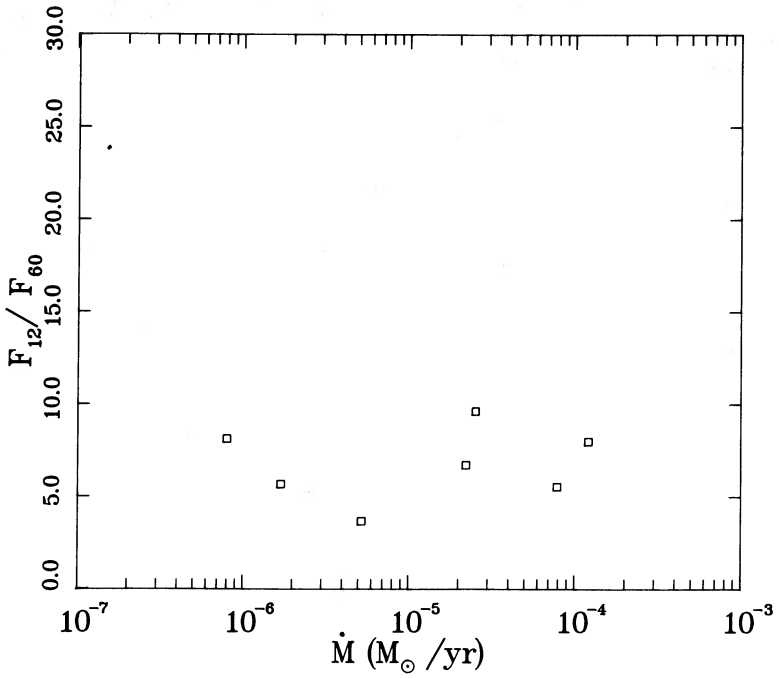

FIG. 4.—Mass-loss rate vs. the 12–60 μm flux (F_ν) ratio

trum (Fig. 2*f*), there is a prominent broad feature at 8 μm which is probably due to a dust feature yet unidentified.

V. DISCUSSION

The color temperatures of the detected sources are generally near 500 K, very similar to the color temperature of IRC +10216. Such low color temperatures suggest that the circumstellar envelopes are optically thick in the near-infrared, a conclusion supported by the high mass-loss rates estimated from the CO antenna temperature. While the light curves of the *IRAS* objects have not been determined, their high probabilities of variability suggest that they are also pulsating as IRC +10216, which has a period of $\sim$600 days.

Figure 5 shows the *IRAS* spectrum of IRC +10216. Its resemblance to our sources is evident. Also plotted are the near-infrared measurements given in Bergeat *et al.* (1976) and McCarthy, Howell, and Low (1980). Although the three sets of measurements were not obtained at the same phase, the combined data points can be reasonably fitted by a blackbody curve. Its color temperature of $\sim$500 K is similar to the other sources. The strength of the 11.3 μm feature is weak $\{\log [(F_\lambda)_{11\ \mu m}/(F_\lambda)_{\text{continuum}}] = 0.19\}$, which could be the result of a slightly higher optical depth. The integrated infrared flux, estimated in the same way as the other sources, is 2.02×10^{-5} ergs cm^{-2} s^{-1}, with an uncertainty of $\sim 0.15 \times 10^{-5}$ ergs cm^{-2} s^{-1}. This implies a bolometric luminosity of 5.3×10^4 $L_\odot$ at the distance of 290 pc, 4 times the mean luminosity of our sample of seven sources, and greater than the luminosity limit for AGB stars.

It is difficult to accept that IRC −10216 is a unique object in the Galaxy. Its 12 μm flux of 4.7×10^4 Jy is, however, 50 times stronger than the next brightest object (23320+4316 = AFGL 3116 = IRC +40540) in the 40–49 LRS class and 1000 times stronger than the average 12 μm flux of the sources in our sample. AFGL 3068, another well-known carbon star, is 70 times weaker than IRC +10216. Even if oxygen-rich stars are included for consideration, the apparent brightness of IRC +10216 is still remarkable. The next brightest object at 12 μm is VY CMa [$F_\nu(12\ \mu m) = 9.9 \times 10^3$ Jy] is a core-burning supergiant and has much higher intrinsic luminosity than AGB stars. The next brightest objects, IK Tau and W Hya, are both oxygen-rich and are 10 times fainter than IRC +10216 at 12 μm.

This implies that there is no other object similar to IRC +10216 within a volume of $[(50)^{1/2} \times 290\ \text{pc}]^3 \approx 8.6\ \text{kpc}^3$, and certainly none with $[(10)^{1/2} \times 290\ \text{pc}]^3 \approx 0.8\ \text{kpc}^3$. In comparison, Thronson *et al.* (1987) derive a surface density of $\sim 6\ \text{kpc}^{-2}$ for carbon stars in the solar neighborhood. It is tempting to consider that the carbon star candidates in our sample are just more distant counterparts of IRC +10216. If IRC +10216 is indeed located at a distance of 290 pc, then the sources in our sample would have distances of $(1000)^{1/2} \times 290\ \text{pc} \approx 9$ kpc, which is clearly unacceptable for the Galactic location of these objects. Conversely, if we adopt an average distance for these objects as 5 kpc, then the distance to IRC +10216 would be $\sim 5 \times (1000)^{-1/2} \approx 150$ kpc. This will reduce the volume of exclusion from 8.6 kpc^3 to 1.2 kpc^3, a much more reasonable value. We note that Zuckerman, Dyck, and Claussen (1986) have also argued that IRC +10216 could be as close as 100–150 pc, based on its low expansion velocity (15 km s^{-1}) in comparison with the expansion velocities observed for stars near the tip of the AGB.

VI. CONCLUSIONS

We have detected circumstellar CO emission from seven sources in the *IRAS* LRS catalog which show the 11.3 μm SiC dust feature. The infrared fluxes of these sources are approximately 10 times weaker than the evolved stars detected to have CO emission (Knapp and Morris 1985; Zuckerman and Dyck 1986) and these new CO sources are probably the most

© American Astronomical Society • Provided by the NASA Astrophysics Data System

1987ApJ...320..825L

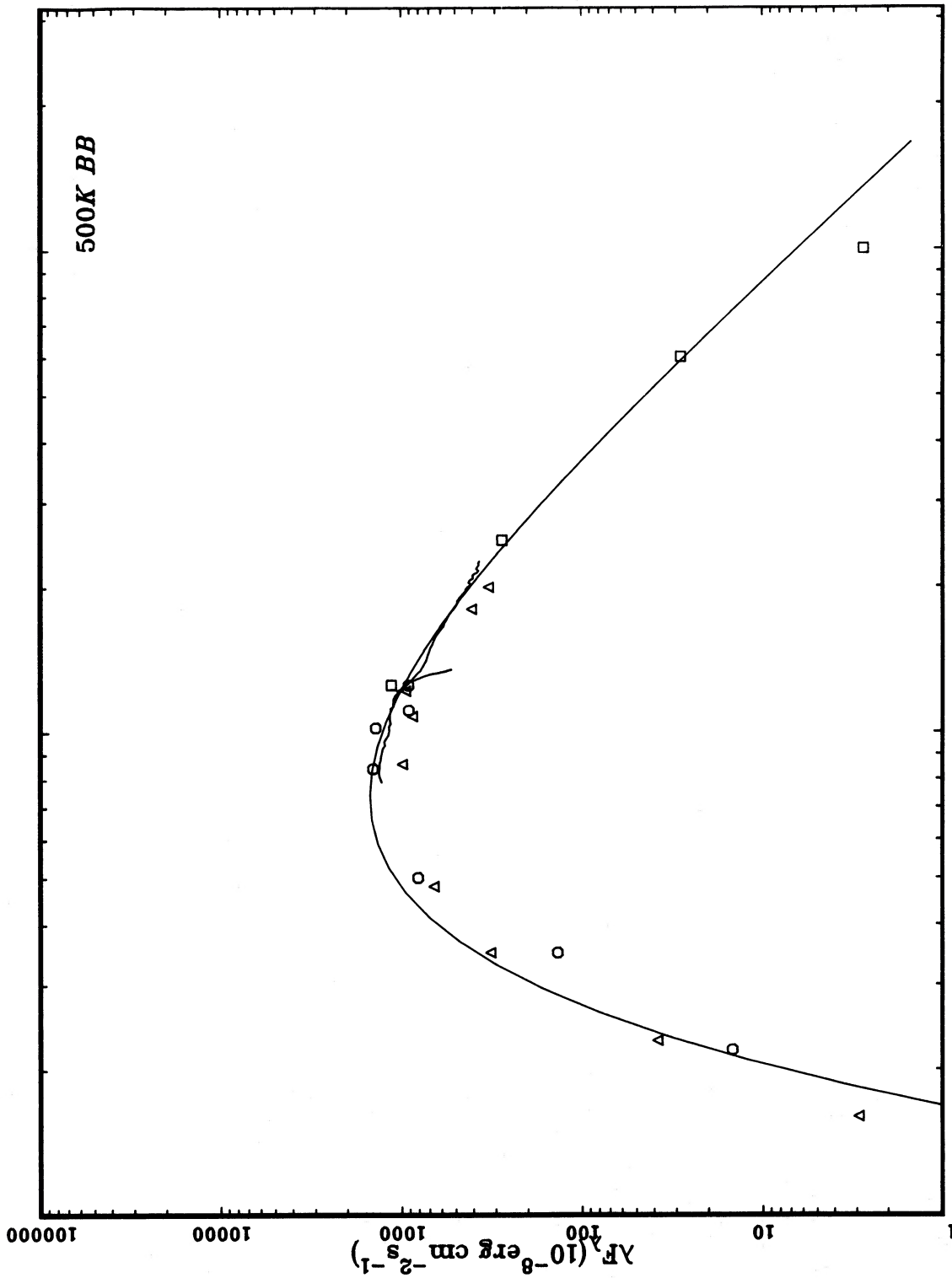

FIG. 5.—The *IRAS* spectrum of IRC +10216. Also plotted are the near-infrared measurements (*circles*) of McCarthy, Howell, and Low (1980), averaged over a period of ~1000 days as given in Gezari, Schmitz, and Mead (1984). Another set of near-infrared measurements compiled by Bergeat *et al.* (1976) is plotted as triangles. The 500 K blackbody curve is normalized with respect to the 60 μm *IRAS* point.

© American Astronomical Society • Provided by the NASA Astrophysics Data System

1987ApJ...320..825L

distant radio carbon stars detected to date. Our results suggest that carbon stars as far as the Galactic center can probably be detected with larger millimeter telescopes such as the IRAM 30 m and the Nobeyama 45 m, where the effects of beam dilution is much reduced.

The infrared spectra of these objects imply color temperatures of ~ 500 K, a value close to that of IRC +10216. The similarities in CO and infrared spectra between IRC +10216, and these sources suggest that they are also carbon stars advanced in the evolution on the AGB. It is only their low color temperatures and low infrared fluxes that have kept them from being discovered earlier. If they are indeed distant counterparts of IRC +10216 then the large apparent brightness of IRC +10216 suggests that it may be closer to the Sun than previously thought.

We thank Dr. P. Jewell of NRAO for valuable assistance during the observing session. The *IRAS Low Resolution Spectra Catalog* is provided on magnetic tape in machine-readable form by the World Data Center in Greenbelt, Maryland. University of Calgary undergraduates G. Young and R. Straker assisted in the analysis of the LRS spectra. The *IRAS* data reduction facility is supported by a grant from the University of Calgary. This work is supported by the Natural Sciences and Engineering Research Council of Canada.

REFERENCES

Bergeat, J., Sibille, F., Lunel, M., and Lefevre, J. 1976, *Astr. Ap.*, **52**, 227.
Burton, W. B. 1974, in *Galactic and Extra-Galactic Radio Astronomy*, ed. G. L. Verschuur and K. I. Kellerman (New York: Springer-Verlag), p. 82.
Gezari, D. Y., Schmitz, M., and Mead, J. M. 1984, *NASA Reference Publication 1118: Catalog of Infrared Observations.*
Gosnel, T. R., Hudson, H., and Puetter, R. C. 1979, *A.J.*, **84**, 538.
Herbig, G. H., and Zappala, 1970, *Ap. J. (Letters)*, **162**, L15.
Hrivnak, B. J., Kwok, S., and Boreiko, R. T. 1985, *Ap. J. (Letters)*, **294**, L113.
IRAS Catalogs and Atlases, Explanatory Supplement. 1985, ed. C. A. Beichman, G. Neugebauer, H. J. Habing, P. E. Clegg, and T. J. Chester (Washington D.C.: U.S. Government Printing Office).
IRAS Science Team. 1986, *Astr. Ap. Suppl.*, **65**, 607.
Knapp, G. R. 1987, in *The Late Stages of Stellar Evolution*, ed. S. Kwok and S. R. Pottasch (Dordrecht: Reidel), in press.
Knapp, G. R., Phillips, J. G., Leighton, R. B., Lo, K. Y., Wannier, P. G., Wootten, H. A., and Huggins, P. J. 1982, *Ap. J.*, **252**, 616.
Knapp, G. R., and Morris, M. 1985, *Ap. J.*, **292**, 640.
Kutner, M., and Ulrich, B. L. 1981, *Ap. J.*, **250**, 341.
Kwan, J., and Hill, F. 1977, *Ap. J.*, **215**, 95.
Kwok, S., Hrivnak, B. J., and Milone, E. F. 1986, *Ap. J.*, **303**, 451.
McCarthy, D. W., Howell, R., and Low, F. J. 1980, *Ap. J. (Letters)*, **235**, L27.
Merrill, K. M., and Ridgway, S. T. 1979, *Ann. Rev. Astr. Ap.*, **17**, 9.
Ney, E. P., and Merrill, K. M. 1980, Study of Sources in AFGL Rocket Infrared Study (AFGL-TR-80-0050).
Olofsson, H. 1987, in *The Late Stages of Stellar Evolution*, ed. S. Kwok, and S. R. Pottasch (Dordrecht: Reidel), in press.
Thronson, H., Latter, W. B., Bally, J., Black, J. H., and Hacking, P. 1987, in *The Late Stages of Stellar Evolution*, ed. S. Kwok and S. R. Pottasch) Dordrecht: Reidel), in press.
Treffers, R., and Cohen, M. 1974, *Ap. J.*, **188**, 545.
Zuckerman, B., and Dyck, M. 1986, *Ap. J.*, **311**, 345.
Zuckerman, B., Dyck, M., and Claussen, M. 1986, *Ap. J.*, **304**, 401.

R. A. ARQUILLA: Computer Science Corporation, Goddard Space Flight Center, Greenbelt, MD 20771

S. KWOK and D. A. LEAHY: Department of Physics, The University of Calgary, Calgary, Alberta, Canada T2N 1N4

© American Astronomical Society • Provided by the NASA Astrophysics Data System